Electrical Power and Energy Systems 169 (2025) 110721

Contents lists available at ScienceDirect

International Journal of Electrical Power and Energy Systems

journal homepage: www.elsevier.com/locate/ijepes

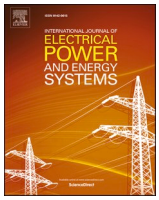

Joint optimization of location and topology of multi-terminal soft open point in distribution networks

Haibo Zhou [a], Guojiang Xiong [a,*], Xiaofan Fu [a,*], Man-Chung Wong [b], Louis-A. Dessaint [c], Kamal Al-Haddad [c]

[a] College of Electrical Engineering, Guizhou University, Guiyang 550025, China
[b] Department of Electrical and Computer Engineering and the State Key Laboratory of Internet of Thing Smart City, University of Macau, Macau
[c] Department of Electrical Engineering, École de Technologie Supérieure, Université du Québec, Montreal H3C 1K3, Canada

ARTICLE INFO

Keywords:
Distribution network
Second-order cone programming
Soft open point
Topology
Location

ABSTRACT

The popularization of renewable energy has led to problems including excessive current and voltage violations in distribution networks. Soft open point (SOP) enables real-time continuous active and reactive power regulation to alleviate these problems. However, how many terminals of a SOP should be set, and which feeders should be interconnected with these terminals is a crucial issue. To address this issue and fully utilize the performance of SOP, this paper conducts a comparative study of SOP with different topologies. First, a nonlinear programming (NLP) model to reveal the effect of multi-terminal SOP (MTSOP) in minimizing system losses and voltage deviation is developed. Second, to facilitate the solution, the NLP model is transformed into a second-order cone programming (SOCP) model based on cone relaxation. Finally, validation on the IEEE 33-, 69- and 141-node systems is conducted. MTSOP can reduce the total losses of IEEE 33-, 69- and 141-node systems by up to 23.54 %, 37.98 %, and 28.90 %, respectively. Although SOPs with a large number of terminals have excellent performance, they are difficult to gain an advantage in feasibility. Therefore, it is not necessarily better to have more terminals in an MTSOP which should be determined based on the characteristics of distribution networks.

1. Introduction

1.1. Motivation

Environmental and policy requirements have greatly affected the energy structure of power distribution system. Many new challenges in the distribution network are caused by the uncertainty of renewable energy (photovoltaics [1], wind turbines [2]), such as deterioration of power quality, frequent voltage fluctuations, network congestion [3]. Although traditional regulation devices possess the ability to reduce network loss and suppress illegal voltage fluctuation, for example capacitor banks (CB) [4] and on-load tap changers (OLTC) [5], they have the limitations of slow response speed and discrete control, which make them cannot effectively tackle the numerous problems brought by renewable energy resources [6]. In recent years, soft open point (SOP) [7,8] has become an effective flexible tool for regulating distribution networks because of its excellent power flow control capability. The main device that makes up the SOP is the voltage source converter (VSC), which is commonly constructed in a back-to-back (B2B) configuration. SOP is ordinarily configured at the end of feeders to provide fast, continuous, and dynamic control involving both active and reactive power flow for optimizing voltage profile and facilitating load balance [9]. Meanwhile, the instant control of the current and the isolation of the DC part enable the SOP to coordinate well with the protection equipment to shorten the fault time in the case of system failure [10]. These advantages make it more convenient to deal with the problems of an active distribution network (ADN) compared to traditional devices. However, the differences in topology and installation location of SOP can affect its power flow control capability. Therefore, it is necessary to compare the performance of SOP with different topologies in the same distribution network operating status, while considering the impact of installation location on SOP, so that SOP can maximize its performance within the candidate place range.

1.2. Literature Review

Previous studies have mainly investigated the control, benefits, planning problems and solution methods of B2B SOP [11–20]. A local control scheme for SOP was proposed to suppress the illegal fluctuations

* Corresponding authors.
E-mail addresses: gjxiongee@foxmail.com (G. Xiong), xffu3@gzu.edu.cn (X. Fu).

https://doi.org/10.1016/j.ijepes.2025.110721
Received 15 October 2024; Received in revised form 17 February 2025; Accepted 30 April 2025
Available online 15 May 2025

Nomenclature

Sets

M_b	Set of branches

Variables

$P_{t,ji}/Q_{t,ji}$	Active/reactive power of branch *ji* within time *t*
$P_{t,i}^{SOP}/Q_{t,i}^{SOP}$	Active/reactive power flowing through the converter at node *i* within time *t*
$P_{t,i}/Q_{t,i}$	Active/reactive power injected into node *i* within time *t*
$V_{t,i}/v_{t,i}$	Voltage amplitude and its square value of node *i* within time *t*
$I_{t,ij}/l_{t,ij}$	Current amplitude and its square value of branch *ij* within time *t*
$\widetilde{V}$	Desired range of voltage amplitude
$P_{t,i}^{SOP,loss}$	Active power losses of SOP at node *i* within time *t*
$Aux_{t,i}$	Voltage deviation auxiliary variable at node *i* within time *t*
$l_{t,new}$	Square value of current flowing through the new transmission line within time *t*
δ	Length of transmission line

Parameters

NT	Total quantity of time periods
NB	Total quantity of nodes
Δt	Span of each time period
r_{ij}/x_{ij}	Resistance/inductance of branch *ij*
$P_{t,i}^{L}/Q_{t,i}^{L}$	Active/reactive load consumption at node *i* within time *t*
A_i^{SOP}/S_i^{SOP}	Loss coefficient/capacity of SOP at node *i*
$V_{des,min}/V_{des,max}$	Minimum/maximum boundary of desired voltage
$V_{i,min}/V_{i,max}$	Minimum/maximum boundary of statutory voltage
$P_{t,i}^{PV}/P_{t,i}^{WT}$	Active power generated by photovoltaics/wind turbine at node *i* within time *t*
$I_{ij,max}$	Upper boundary of current amplitude of branch *ij*
m	Number of SOP's terminals
y	Economical service life of MTSOP
ε	Coefficient of MTSOP annual operational cost
d	Discount rate
c^E	Electricity price
c^{SOP}	Unit capacity cost of MTSOP
c^L	Construction cost per unit length of transmission lines
β	Line resistance value per unit length

of voltage while integrating renewable energy resource into the distribution network [11]. For active/reactive power flow control, one of the SOP's converters usually uses the Vdc-Q control strategy and the other converters adopt the P-Q control strategy [12]. In [13], the authors confirmed that the failure recovery capability of the distribution system could be enhanced by the remote-controlled switch and SOP. Zhang etc. [14] proposed SOP-based distribution service restoration (DSR) models by considering voltage deviation, power loss and load restoration, and the results showed that SOP-based DSR strategies could effectively improve power supply restoration capability. Li etc. [15] proposed a self-healing power restoration method based on multiple SOPs, which could improve the load restoration level of AND by using the metrics of power restoration, system loss and switching operation cost. Ji etc. [16] developed a SOP-based AND time series islanding model with the objective of power supply restoration, which exploited the flexibility of SOP's power control capability to improve load recovery. In [17], an optimal planning model concerning SOP was proposed, and the results showed that as the SOP's capacity increased, the SOP's capability of reducing power losses and supply recovery would reach its limit. In [18], a bi-level planning model was proposed to not only plan the size and placement of SOP and distributed generation (DG), but also improve the operational status of the entire system. To quantify the capacity of SOP, a method based on reliability was presented to relax the capacity model to a second-order cone programming (SOCP) for shorter computation time [19]. In [20], an advanced iterative cut plane (ICP) method was proposed to make the semi-definite relaxation model more accurate in optimizing the operating state of SOP. In summary, the introduction of SOPs can effectively improve power quality, mitigate voltage fluctuations, improve the solution method, and enhance the reliability and economy of ADNs.

In addition to the research on SOP's regulation capability, the effect of location and topology of SOP has also gained attention. In [7], different installation quantities of SOP were compared from the perspectives of load balancing and voltage profile, and the results showed that when the installation quantity was too large, the performance of SOP would decrease. In [21], a multi-terminal SOP (MTSOP) structure

TABLE 1
Recent Research on the Topology, Quantity, and Location of SOP.

Ref.	Optimization objective	SOP		
		Topology	Quantity	Maximum number of candidate places
[7]	Load balance index	2-termianl	0, 1, 2, 3, 4	8
[8]	Power losses, aggregate voltage deviation index, total harmonic distortion	2-termianl	0, 1	10
[9]	Annual investment planning cost, operating cost	2-terminal	1, 2	20
[10]	Capital cost of SOP, annual operational cost of SOP, annual energy loss cost	2-terminal	0, 1, 3, 5	26
[13]	Annual co-deployment cost, cost of lost loads	2-terminal	0, 1, 2, 3, 4, 5	10
[14]	Load restoration, voltage deviation, power losses	2-terminal	0, 2	4
[15]	Active power of restored loads, cost of power loss and switching operation	2-terminal	0, 2, 5	10
[16]	Active power of restored loads	2-terminal	0, 2	4
[17]	Power losses	2-terminal	1, 2	4
[18]	Total annual costs, power loss, voltage negative sequence unbalance	2-terminal	0, 1	26
[19]	Substation demand	2-ternimal	5	10
[20]	Total system loss, voltage amplitude unbalance	5-terminal	0, 1	5
[23]	Energy loss, feeder load balancing, voltage profile	2-terminal 3-terminal	0, 1	3
[27]	Total operational cost, voltage deviation	2-terminal	0, 2	4
This work	Operating losses, voltage deviation	2-terminal 3-terminal 4-ternimal 5-terminal 6-ternimal	0, 1, 2, 3	6

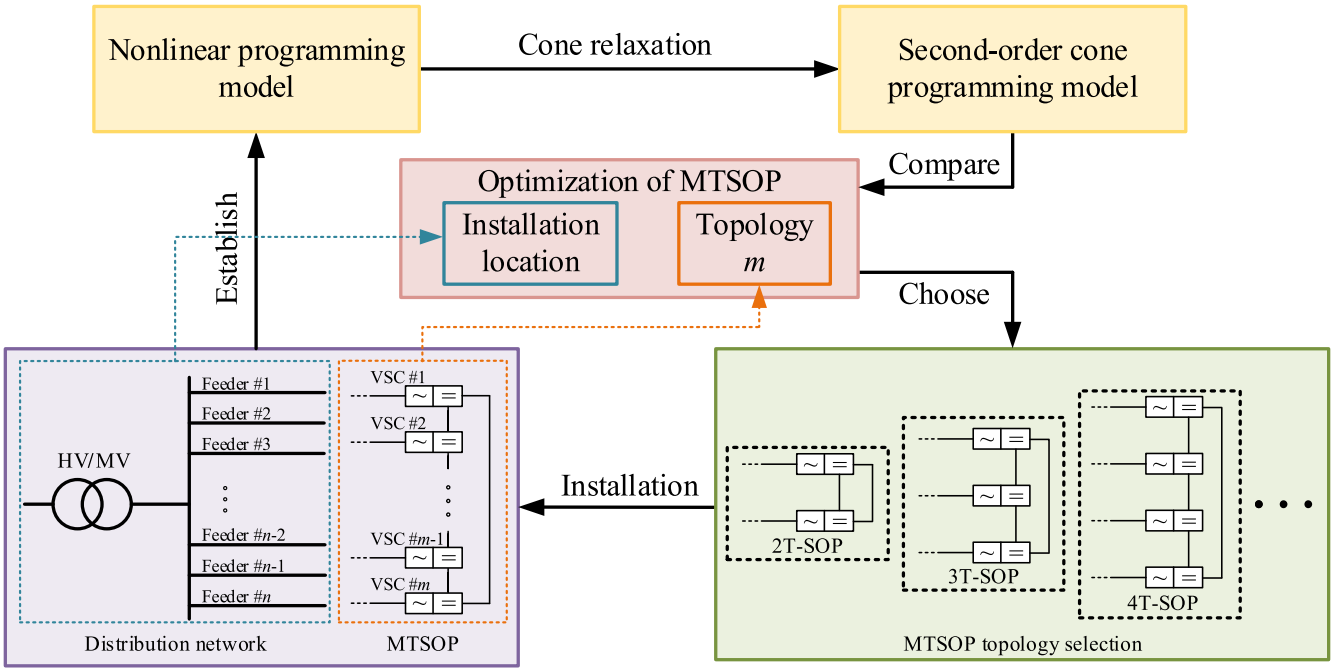

Fig. 1. MTSOP topology comparison study framework.

was proposed, which could save numerous passive components and switching devices, making the SOP compact in structure, low in cost, and small in size. Taher etc. [22] proposed a multi-terminal SOP with energy storage elements as a potential solution to the load frequency control problem. They also proposed a hybrid jellyfish search and particle swarm optimization algorithm to enhance the performance of MTSOP. In [23], by comparing the effect of two-terminal and three-terminal topologies on reducing network losses and maintaining voltage balance, it was concluded that the three-terminal topology performs better. Table 1 summarizes the above studies in terms of topology and location of SOP. The current researches mainly focus on two-terminal and three-terminal SOPs. In [24], an MTSOP with over three terminals was proposed, which could allow for better regulation by interconnecting multiple feeders simultaneously. However, increasing the number of MTSOP's terminals will greatly increase the complexity of coordinated control among feeders.

1.3. Research gaps

The studies in Table 1 mainly considered the SOP with B2B topology and optimizing the system by increasing the number of 2-terminal SOPs while ignoring the scheme of MTSOP in the face of a larger scale distribution network or multiple feeders that need to be interconnected. There are two research gaps in SOP's topology. One is how the impact of SOP on the distribution network changes as the number of SOP's terminals increases. The second is to use multiple 2-terminal SOPs or one MTSOP scheme when interconnecting multiple feeders, which scheme is more effective.

1.4. Contributions

In order to make up for the lack of current research in MTSOP topology optimization, this paper conducts a comparative study of distribution network optimization models based on different topologies of MTSOP, and analyzes the impacts brought by the topological differences of MTSOP, as shown in Fig. 1. For a distribution network, how many terminals of an MTSOP are needed and where each terminal is connected deserves a deeper study, since both location and topology affect its size, cost, and performance. This study develops a nonlinear programming (NLP) model to jointly optimize both the location and topology of MTSOP by minimizing the overall operating losses and voltage deviation. Relaxation technique is applied to this model to facilitate the solution by drawing support from the SOCP [25,26]. The model is demonstrated in IEEE 33-, 69-, and 141-node systems. The main contributions of this paper include:

1) In order to study the impact of MTSOP topology on its power flow control capability, this paper extends the number of terminals of MTSOP to 6, and comprehensively analyzes the performance of MTSOP with different topologies at the end of different sizes of distribution networks.
2) In the case where the distribution network needs to interconnect 3 feeders and above, two schemes are adopted. One is to interconnect by increasing the number of 2-terminal SOPs. The second is to use MTSOP for interconnection. These two schemes are measured by comparing the differences in total system losses and voltage quality for the same VSC capacity, load, and power scenarios, which fills the gap in current research that lacks a comparison of the effects of these two schemes.
3) The objective is to jointly optimize the topology and location of MTSOP for the feeder ends of distribution networks with varying sizes. Considering the feasibility and optimization results, the optimal configuration of MTSOP is selected in order to ensure that it functions to the greatest extent possible.

The rest is structured below. In Section II, the NLP model is developed. Linearization and cone relaxation are adopted to transform the NLP model in Section III. In Section IV, three testing systems are applied to validate the proposed model. Section V summarizes this paper.

2. Optimization model of MTSOP

SOP can perform real-time active/reactive power regulation to reduce power loss. In this work, an NLP model is constructed to decrease the system operation cost and mitigate the voltage deviation by optimizing the operation of MTSOP. The MTSOP is mostly installed at the end of feeders to exert its strong power flow control capability. Compared with the B2B SOP, the MTSOP is more advantageous in

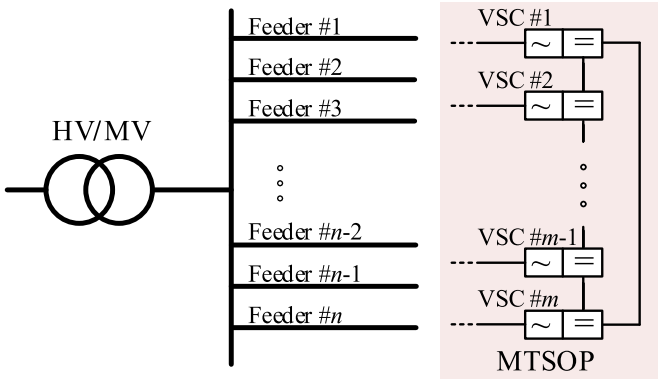

Fig. 2. MTSOP in a distribution network.

solving the problems of voltage overrun at the end of long feeders, unbalanced power flow, excessive network losses, and power restoration after faults. Of course, this does not mean that more terminals are better, and increasing the number of terminals will make the control more complicated [24] and more expensive. Thus, it is necessary to optimize the number of terminals. For a distribution network with n feeders and an MTSOP with m terminals shown in Fig. 2, how large the number m should be set and which feeders should be interconnected with these m terminals to make the system operate more efficiently is the focus of this work.

2.1. Optimization objectives

Since the MTSOP can improve the operating efficiency and voltage balance of distribution network, the objectives are to minimize both operating losses and voltage deviation. The overall operating losses are induced by feeder lines and MTSOP, as given by:

$$f_{TL} = \sum_{t=1}^{NT} \sum_{ij \in M_b} r_{ij} I_{t,ij}^2 \Delta t + \sum_{t=1}^{NT} \sum_{i=1}^{NB} P_{t,i}^{SOP,loss} \Delta t \tag{1}$$

where r_{ij} is the resistance of branch ij. The $I_{t,ij}$ is the current amplitude of branch ij within time t. The Δt is the span of each time period. The $P_{t,i}^{SOP,loss}$ is the active power losses of SOP.

The voltage deviation f_V is provided by:

$$f_V = \sum_{t=1}^{NT} \sum_{i=1}^{NB} \left| V_{t,i}^2 - \widetilde{V}^2 \right| : \left(V_{t,i} \geq V_{des,max} \middle| \middle| V_{t,i} \leq V_{des,min} \right) \tag{2}$$

where $V_{t,i}$ is the voltage amplitude, and $\widetilde{V}$ is the Desired range of voltage amplitude. The $V_{des,min}$ and $V_{des,max}$ are the minimum and maximum boundary of desired voltage.

The above two sub-objectives can be merged to form the final objective function:

$$\min f = \lambda_L \cdot f_{TL} + \lambda_V \cdot f_V \tag{3}$$

The weight coefficients λ_L and λ_V can be set according to the analytic hierarchy process (AHP) [27,28].

2.2. Constraints

The DistFlow model [29] is utilized and can be described by:

$$\sum_{ji \in M_b} \left(P_{t,ji} - r_{ji} I_{t,ji}^2 \right) + P_{t,i} = \sum_{ik \in M_b} P_{t,ik} \tag{4}$$

$$\sum_{ji \in M_b} \left(Q_{t,ji} - x_{ji} I_{t,ji}^2 \right) + Q_{t,i} = \sum_{ik \in M_b} Q_{t,ik} \tag{5}$$

$$V_{t,i}^2 - V_{t,j}^2 - 2\left(r_{ij} P_{t,ij} + x_{ij} Q_{t,ij} \right) + \left(r_{ij}^2 + x_{ij}^2 \right) I_{t,ij}^2 = 0 \tag{6}$$

$$I_{t,ij}^2 V_{t,i}^2 = P_{t,ij}^2 + Q_{t,ij}^2 \tag{7}$$

$$P_{t,i} = P_{t,i}^{PV} + P_{t,i}^{WT} + P_{t,i}^{SOP} - P_{t,i}^{L} \tag{8}$$

$$Q_{t,i} = Q_{t,i}^{SOP} - Q_{t,i}^{L} \tag{9}$$

where, $P_{t,ji}$ and $Q_{t,ji}$ are the active and reactive power of branch ji. The x_{ij} is the inductance of branch ij. $P_{t,i}$ and $Q_{t,i}$ are the active and reactive power injected into node i. $P_{t,i}^{PV}$ and $P_{t,i}^{WT}$ are the active power generated by photovoltaic (PV) and wind turbine (WT) at node i within time t. $P_{t,i}^{SOP}$ and $Q_{t,i}^{SOP}$ are the active and reactive power flowing through the converter connected to node i within time t. $P_{t,i}^{L}$ and $Q_{t,i}^{L}$ are the active and reactive load consumption.

The voltage and current must be within the allowable ranges.

$$V_{i,min}^2 \leq V_{t,i}^2 \leq V_{i,max}^2 \tag{10}$$

$$I_{t,ij}^2 \leq I_{ij,max}^2 \tag{11}$$

The MTSOP must satisfy the following constraints:

$$\sum_{i=1}^{m} \left(P_{t,i}^{SOP} + P_{t,i}^{SOP,loss} \right) = 0 \tag{12}$$

$$P_{t,i}^{SOP,loss} = A_i^{SOP} \sqrt{\left(P_{t,i}^{SOP} \right)^2 + \left(Q_{t,i}^{SOP} \right)^2} \tag{13}$$

$$Q_{i,min}^{SOP} \leq Q_{t,i}^{SOP} \leq Q_{i,max}^{SOP}, i \in \{1, 2, \ldots, m\} \tag{14}$$

$$\sqrt{\left(P_{t,i}^{SOP} \right)^2 + \left(Q_{t,i}^{SOP} \right)^2} \leq S_i^{SOP}, \ i \in \{1, 2, \ldots, m\} \tag{15}$$

where, A_i^{SOP} and S_i^{SOP} are the loss coefficient and capacity of SOP. $Q_{i,min}^{SOP}$ and $Q_{i,max}^{SOP}$ are the minimum and maximum boundary of the reactive power flowing through the converter connected to node i.

The variables of this model involve the continuous variables of MTSOP's active/reactive power output.

3. Model conversion

3.1. Standard form of SOCP

The proposed NLP model is hard to solve effectively. Here, the SOCP technique is applied to facilitate the solution. The SOCP, as an extension of linear and nonlinear programming, is a convex programming method [30,31]. Its standard format is:

$$\min \left\{ c^T z | Nz = b, z \in D \right\} \tag{16}$$

where z denotes the decision variable; c and b represent constant vectors;N represents a constant matrix; D is given by a quadratic cone (17) or a rotated quadratic cone (18):

$$D_1 = \left\{ z \in R^n : z_1 \geq \sqrt{\sum_{j=2}^{n} z_j^2}, z_1 \geq 0 \right\} \tag{17}$$

$$D_2 = \left\{ z \in R^n : 2 z_1 z_2 \geq \sum_{j=3}^{n} z_j^2, z_1, z_2 \geq 0 \right\} \tag{18}$$

To sum up, there are rigorous requirements for expressing SOCP in mathematical form. The form is required to be linear, and its feasible domain includes convex cone constraints and linear equality constraints.

Thus, the initial NLP model to reduce system losses and voltage deviation needs to be linearized and relaxed to facilitate the solution.

3.2. Model Conversion technique

There are many nonlinear terms in the initial model, including the square form of the current and voltage amplitudes. Let $l_{t,ij}$ and $v_{t,i}$ represent $I^2_{t,ij}$ and $V^2_{t,i}$, so (1), (4)–(6), (10) and (11) can be linearized as [27]:

$$f_{TL} = \sum_{t=1}^{NT} \sum_{ij \in M_b} r_{ij} l_{t,ij} \Delta t + \sum_{t=1}^{NT} \sum_{i=1}^{NB} P_{t,i}^{SOP,loss} \Delta t \tag{19}$$

$$\sum_{ji \in M_b} \left(P_{t,ji} - r_{ji} l_{t,ji}\right) + P_{t,i} = \sum_{ik \in M_b} P_{t,ik} \tag{20}$$

$$\sum_{ji \in M_b} \left(Q_{t,ji} - x_{ji} l_{t,ji}\right) + Q_{t,i} = \sum_{ik \in M_b} Q_{t,ik} \tag{21}$$

$$v_{t,i} - v_{t,j} - 2\left(r_{ij} P_{t,ij} + x_{ij} Q_{t,ij}\right) + \left(r_{ij}^2 + x_{ij}^2\right) l_{t,ij} = 0 \tag{22}$$

$$V^2_{i,min} \le v_{t,i} \le V^2_{i,max} \tag{23}$$

$$l_{t,ij} \le I^2_{ij,max} \tag{24}$$

The (7), after replacing $V^2_{t,i}$ and $I^2_{t,ij}$, is still nonlinear and further cone relaxation is required.

$$\left\| \begin{matrix} 2P_{t,ij} \\ 2Q_{t,ij} \\ l_{t,ij} - v_{t,i} \end{matrix} \right\|_2 \le l_{t,ij} + v_{t,i} \tag{25}$$

The (13) and (15) can be relaxed to the form of rotational quadratic cone constraints (26) and (27).

$$\left(P_{t,i}^{SOP}\right)^2 + \left(Q_{t,i}^{SOP}\right)^2 \le 2 \frac{P_{t,i}^{SOP,loss}}{\sqrt{2} A_i^{SOP}} \frac{P_{t,i}^{SOP,loss}}{\sqrt{2} A_i^{SOP}} \tag{26}$$

$$\left(P_{t,i}^{SOP}\right)^2 + \left(Q_{t,i}^{SOP}\right)^2 \le 2 \frac{S_i^{SOP}}{\sqrt{2}} \frac{S_i^{SOP}}{\sqrt{2}} \tag{27}$$

The voltage deviation (2) needs to be linearized by introducing a new auxiliary variable $Aux_{t,i}$ as:

$$f_V = \sum_{t=1}^{NT} \sum_{i=1}^{NB} \left(Aux_{t,i}\right) \tag{28}$$

The auxiliary variables need to satisfy (29), (30), and (31):

$$Aux_{t,i} \ge v_{t,i} - V^2_{des.max} \tag{29}$$

$$Aux_{t,i} \ge -v_{t,i} + V^2_{des.min} \tag{30}$$

$$Aux_{t,i} \ge 0 \tag{31}$$

Hence, the initial model is transformed into a SOCP model.

$$\begin{aligned} &\min f = \lambda_L f_{TL} + \lambda_V f_V \\ &\text{s.t.} \begin{cases} (8), (9), (12) \\ (14), (19) - (31) \end{cases} \end{aligned} \tag{32}$$

For the SOCP model above, vital inputs include line and load parameters as well as the power generated from wind turbines, photovoltaics. The outputs include the operations of MTSOP, voltage deviation, and power flow.

4. Feasibility analysis

The feasibility analysis considers the following factors. The installation of MTSOP in the distribution network requires new transmission lines (here we ignore other devices). Over the service life of the MTSOP, the scheme is considered to be feasible if the reduction in the electricity cost due to the system losses' reduction is greater than the construction cost of both transmission lines and MTSOP and the operating cost of the MTSOP, that is:

$$C^{RE} - C^{LINE} - C^{MT} - C^{OPE} \ge 0 \tag{33}$$

where C^{RE} denotes the reduced cost due to lower system losses. C^{LINE} and C^{MT} are the construction cost of transmission lines and MTSOP. The C^{OPE} is the operating cost of MTSOP throughout its service life. The δ is the length of new transmission lines. The items in (33) are calculated as follows:

1) Reduced cost C^{RE} due to lower system losses:

$$C^{RE} = 365 \cdot y \cdot c^E \cdot \left(P_{loss,before} - \left(P_{loss,after} + P_{loss,new}\right)\right) \tag{34}$$

where y denotes the service life of the MTSOP. The c^E is the price of electricity. $P_{loss,before}$ and $P_{loss,after}$ denote the daily total losses of the distribution network without and with the MTSOP, respectively. $P_{loss,new}$ denotes the daily power loss of the new transmission lines.

$$P_{loss,new} = \sum_{t=1}^{NT} \delta \cdot \beta \cdot l_{t,new} \cdot \Delta t \tag{35}$$

where δ is the length of the transmission lines. β is the resistance of the transmission lines per kilometer, and $l_{t,new}$ is the square value of the current flowing through the new transmission lines at time t.

2) Transmission lines' construction cost C^{LINE}:

$$C^{LINE} = c^L \cdot \delta \tag{36}$$

where c^L is the construction cost per unit length of the transmission lines.

3) Construction cost C^{MT} of the MTSOP:

$$C^{MT} = \frac{d \cdot (1+d)^y}{(1+d)^y - 1} \sum_{i=1}^{m} c^{SOP} \cdot S_i^{SOP} \tag{37}$$

where d denotes the discount rate. c^{SOP} is the cost per unit of the MTSOP's capacity.

4) Total operating cost of MTSOP:

$$C^{OPE} = y \cdot \varepsilon \cdot \sum_{i=1}^{m} c^{SOP} \cdot S_i^{SOP} \tag{38}$$

where ε is the coefficient of MTSOP's annual operating cost.

The above parameters are listed in the Table 2.

TABLE 2
Parameters for Feasibility Analysis.

Parameter	Value
y	30.00 years
ε	0.01
d	0.08
c^E	0.08 $/kWh
c^{SOP}	308.80 $/kVA
c^L	30599.80 $/km
β	0.91 Ω/km

5. Case study

Modified IEEE 33–, 69-, and 141-node system were applied to test the developed SOCP model solved by GUROBI in YALMIP at MATLAB R2019b.

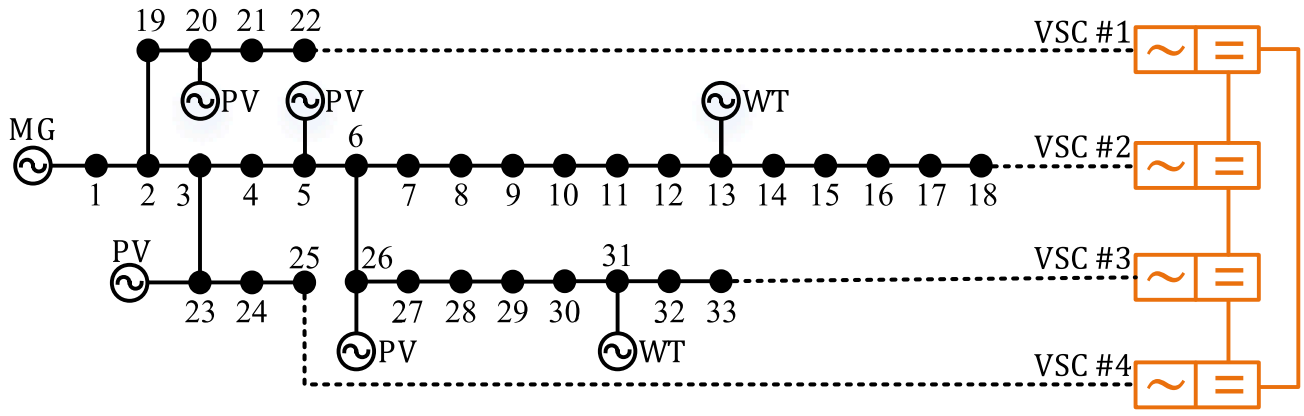

Fig. 3. Topology of MTSOP in IEEE 33-node system.

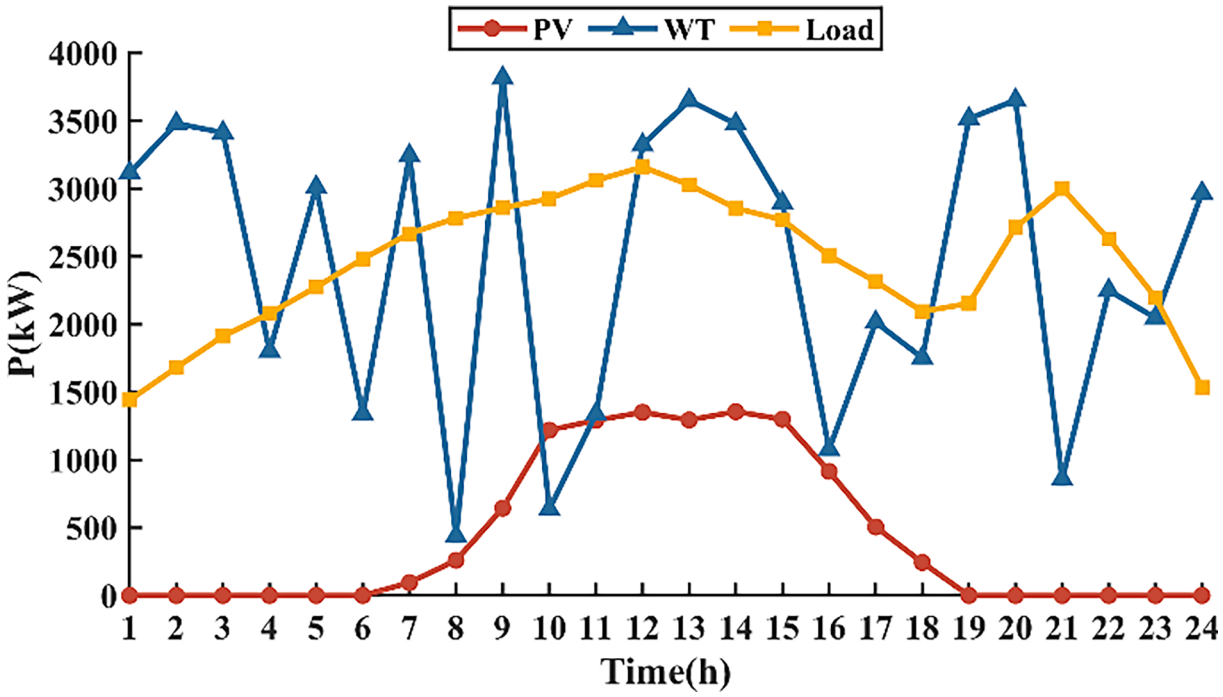

Fig. 4. Power variation of generators and load.

TABLE 3
Installation Locations of MTSOP in IEEE 33-Node System.

Scenario	I	II	III	IV	V
MTSOP location	–	18–22	18–22–25	18–22–25–33	18–22&25–33
	–	18–25	18–22–33	–	18–25&22–33
	–	18–33	18–25–33	–	18–33&22–25
	–	22–25	22–25–33	–	–
	–	22–33	–	–	–
	–	25–33	–	–	–

5.1. Modified IEEE 33-Node system

As given in Fig. 3, all renewable energy resources operate in unit power factor and their reactive power compensation capabilities are not considered. The main grid (MG) is connected to node 1. The Power variation of generators and load are shown in Fig. 4. The candidate installation locations of MTSOP are the nodes 18, 22, 25, and 33. Each converter of the MTSOP has a capacity of 500kVA and a loss factor of 0.02. The weight parameters λ_V and λ_L are ultimately given as 0.2583 and 0.7417, respectively. The statutory and desired voltage ranges are 0.95 ~ 1.05 p.u. and 0.98 ~ 1.02 p.u., respectively.

To reveal the influence of MTSOP on the system losses and voltage deviation, five scenarios are considered:

Scenario I: No MTSOP is applied in the network.
Scenario II: One 2-terminal SOP is used for regulation.
Scenario III: One 3-terminal SOP is used for regulation.
Scenario IV: One 4-terminal SOP is used for regulation.
Scenario V: Two 2-terminal SOPs are used for regulation.

Table 3 presents the possible installation locations of MTSOP in Scenarios I to V. The optimal installation schemes are selected for comparison in each scenario. The system losses and objective function values of Scenarios I to V are shown in Fig. 5. The voltage distribution is depicted in Figure S1 in Appendix A. Obviously, in the same scenario, the installation location has significant impact on the performance of MTSOP. In Fig. 5, the installation scheme 22–25 in Scenario II has the lowest SOP loss of 0.1712 MW, but the system loss is still high. On the contrary, although the SOP loss of the installation scheme 22–33 is higher at 0.3050 MW, the line loss is lower, leading to lower total losses. In Figure S1(b), the three installation schemes including 18–22, 18–25,

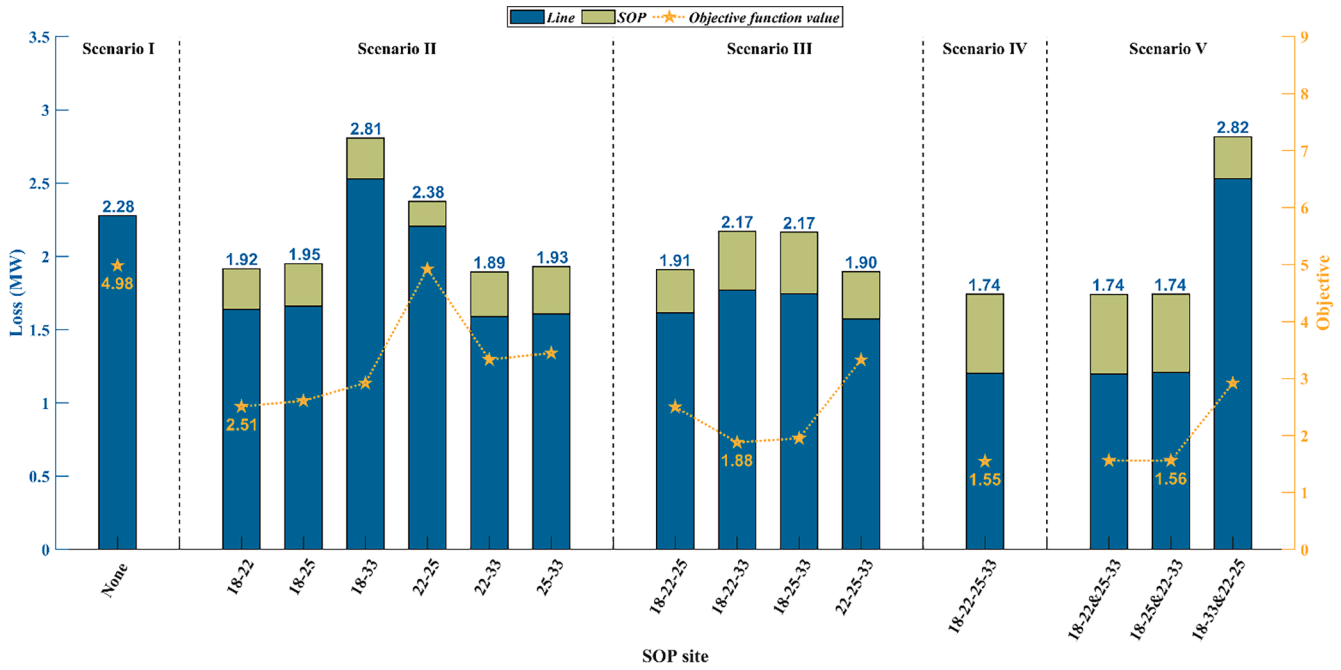

Fig. 5. Total losses and objectives in IEEE 33-node system.

TABLE 4
Results of the Optimal Installation Scheme in IEEE 33-Node System.

Scenario	MTSOP location	Objective function	Total losses (MW)	Line loss (MW)	MTSOP loss (MW)	Voltage deviation (p.u.)
I	–	4.9835	2.2782	2.2782	0.0000	12.7515
II	18–22	2.5078	1.9167	1.6381	0.2786	4.2052
III	18–22–33	1.8800	2.1717	1.7700	0.4017	1.0423
IV	18–22–25–33	1.5483	1.7420	1.2022	0.5398	0.9920
V	18–25&22–33	1.5597	1.7423	1.2085	0.5338	1.0354

and 18–33 are superior at the voltage deviation. The scheme 18–33 obtains better voltage quality at the cost of higher losses. In Scenario III, the objective function value of the scheme 22–25–33 is worse than the other three schemes. In Scenario IV, the scheme 18–22–25–33 has the lowest total system losses at 1.7420 MW and the optimal voltage distribution. In Scenario V, the scheme 18–33&22–25 not only has the highest losses at 2.8167 MW but also greater voltage fluctuations than other two schemes. This means that the installation location has a significant impact on the performance of the SOPs. In addition, the installation schemes with node 18 in Scenario II and Scenario III are superior to other schemes without node 18 in objective function values. This indicates that node 18 is easier to leverage MTSOP's capabilities than other candidate installation locations. In order to reveal the impact of MTSOP's installation location, the optimal scheme of each scenario is selected for comparison, which includes 18–22, 18–22–33, and 18–25&22–33 in Scenarios II, III, and V, respectively.

From the results of optimal installation schemes in Scenarios I to V in Table 4, the following conclusions can be drawn:

1) Compared to Scenario I, the optimal installation schemes for Scenarios II, III, IV, and V show a decrease in the objective values by 49.68 %, 62.28 %, 68.93 %, and 68.70 %, a decrease in the total losses by 15.87 %, 4.67 %, 23.54 %, and 23.52 %, and in the voltage deviations by 67.02 %, 91.83 %, 92.22 % and 91.88 % respectively. As the number of MTSOP's terminals increases, the voltage deviation of the system can be continuously improved but the total loss may not be continuously reduced. This is because increasing the number of MTSOP's terminal will increase its own loss, which requires that MTSOP must further improve the power flow distribution to obtain a lower total system loss. In Figure S1, the optimal voltage distribution for each scenario is similar, and increasing the number of SOP's terminals can only slightly improve the voltage distribution. This is mainly because when the system approaches the ideal status, there is limited room for improvement in node voltage, and increasing the number of SOP's terminals results in less voltage improvement. Besides, the 4-terminal SOP scheme has the optimal objective value for all scenarios with optimal total system loss and voltage quality, which demonstrates the potential performance advantage of MTSOP. Moreover, the performance of MTSOP is influenced by topology and location. Therefore, the optimal scheme for Scenario III achieves a lower voltage deviation at the expense of higher losses compared to Scenario II.
2) When four feeders need to be interconnected, scheme 18–22–25–33 dominates with a total loss of 1.7420 MW, and its voltage deviation is 4.19 % lower than that of scheme 18–25&22–33. The main factor is that interconnecting all feeders simultaneously makes the power flow more rational. Hence, the topology of MTSOP with multiple feeders interconnected simultaneously is better in improving the system's operating status.

It is worth noting that there are relatively small errors among the solutions of the relaxed model (SOCP) and the initial model (NLP), which is mainly caused by the introduction of second-order cone relaxation. Studies have shown that when the accuracy requirement is not particularly high, the relaxation can achieve sufficient accuracy [32]. To analyze the impact on the solution accuracy, the error induced by relaxation of equality constraint (7) to inequality constraint (25) can be expressed as the following infinite norm (39).

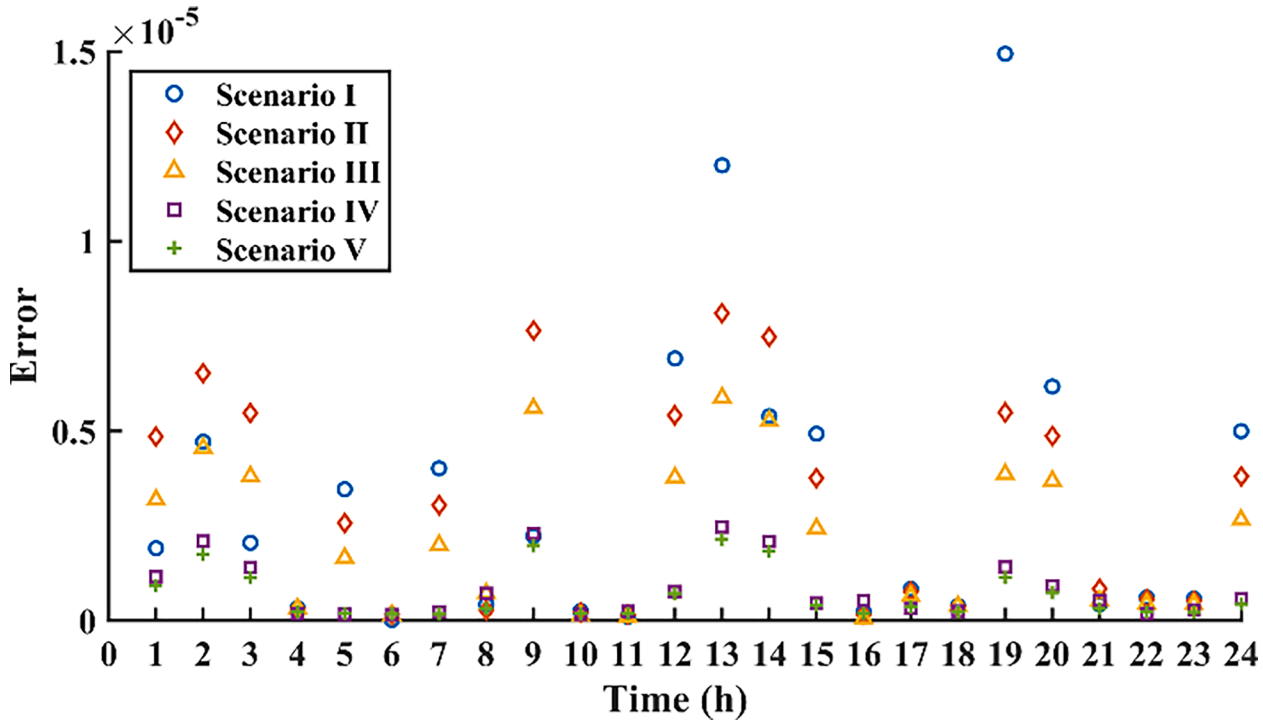

Fig. 6. Maximum errors in optimal installation schemes of Scenarios I to V (IEEE 33-node system).

TABLE 5
Results of Feasibility in IEEE 33-node system.

MTSOP location	C^{RE}($)	C^{LINE}($)	C^{MT}($)	C^{OPE}($)	δ(km)
18–22	254241	134171	27430	92640	4.3847
18–22–33	121373	−58732	41145	138960	−1.9194
18–22–25–33	395512	155372	54860	185280	5.0776
18–25&22–33	396174	156034	54860	185280	5.0992

$$error = \left\| l_{t,ij} - \frac{P_{t,ij}^2 + Q_{t,ij}^2}{v_{t,i}} \right\|_\infty \tag{39}$$

The maximum errors in optimal installation schemes of Scenarios I to V are shown in Fig. 6. These maximum errors are all with a 1.0e-5 level. Therefore, the relaxed model SOCP can be considered accurate.

The length of transmission lines that can be built is constrained by the feasibility (33). The δ can be regarded as the longest transmission line planned to be constructed by the scheme. The feasibility (33) can be further interpreted to mean that the scheme is feasible when the actual length of transmission line to be constructed is less than the δ. Table 5 shows the maximum length of transmission lines that can be built for each scheme. Scheme 18–22–33 satisfies (33) when the length of the line is negative, which means that this scheme is not feasible. The schemes 18–22, 18–22–25–33 and 18–25&22–33 are feasible when the actual transmission lines to be constructed are less than 4.38 km, 5.08 km and 5.10 km respectively. When the δ is larger, the feasibility of the scheme is greater. Schemes 18–22–25–33 and 18–25&22–33 have similar feasibility due to the close cost of SOP and system losses. Scheme 18–22 is feasible due to the lower cost of the SOP although the performance of the SOP is weaker. Which scheme can be implemented will be influenced

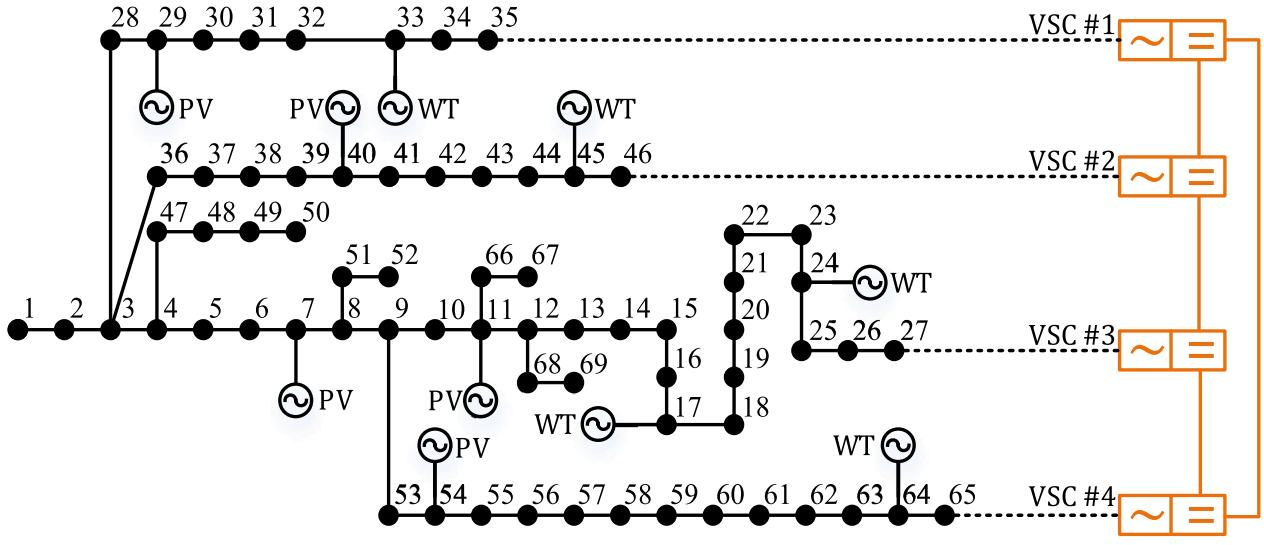

Fig. 7. Topology of MTSOP in IEEE 69-node system.

TABLE 6
Installation Locations of MTSOP in IEEE 69-Node System.

Scenario	I	II	III	IV	V
MTSOP location	–	27–35	27–35–46	27–35–46–65	27–35&46–65
	–	27–46	27–35–65	–	27–46&35–65
	–	27–65	27–46–65	–	27–65&35–46
	–	35–46	35–46–65	–	–
	–	35–65	–	–	–
	–	46–65	–	–	–

by a number of factors such as performance, geographic location, budget, etc., and will be the subject of future research.

5.2. Modified IEEE 69-Node system

This case, as given in Fig. 7, is utilized for verifying the extensibility of the proposed method. It contains five wind turbines and five photovoltaic plants. Node 1 is the slack bus. The range of desired voltage is 0.97 ~ 1.03 p.u. and each converter of the MTSOP has a capacity of 1MVA. Nodes 27, 35, 46, and 65 are the candidate installation locations of MTSOP. The rest parameters adopt the same values in the previous system. Table 6 shows the installation locations of MTSOP in all scenarios.

Fig. 8 illustrates that the effect of MTSOP is affected by its topology and installation location. Node 65 is easier to leverage the effect of MTSOP compared to other candidate installation locations. The optimal MTSOP's installation schemes of Scenarios II, III, and V are 46–65, 27–46–65, and 27–35&46–65, respectively. In Figure S2 in Appendix A, their maximum and minimum node voltages at each time period almost meet the desired voltage range. The solutions of the optimal installation schemes are tabulated in Table 7 and their maximum errors are shown in Fig. 9. From the perspective of error, these maximum errors are all at the level of 1.0e-5, so the accuracy is acceptable. Compared to Scenario I, the optimal schemes for Scenarios II, III, IV, and V show a decrease of 69.18 %, 71.59 %, 71.69 %, and 69.20 % in the objective values and a decrease of 32.20 %, 37.77 %, 37.98 %, and 32.17 % in the total loss. This indicates that increasing the number of MTSOP's terminals can indeed improve the operational level of the distribution network. Obviously, the scheme 27–35–46–65 with a total loss of 1.5423 MW and a voltage deviation of 0.0702 outperforms all other schemes for this

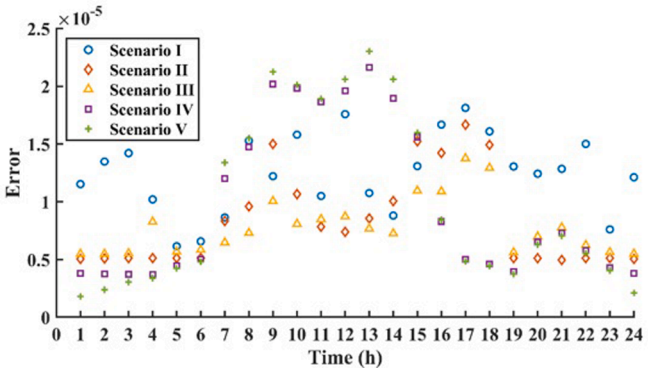

Fig. 9. Maximum errors in optimal installation schemes of Scenarios I to V (IEEE 69-node system).

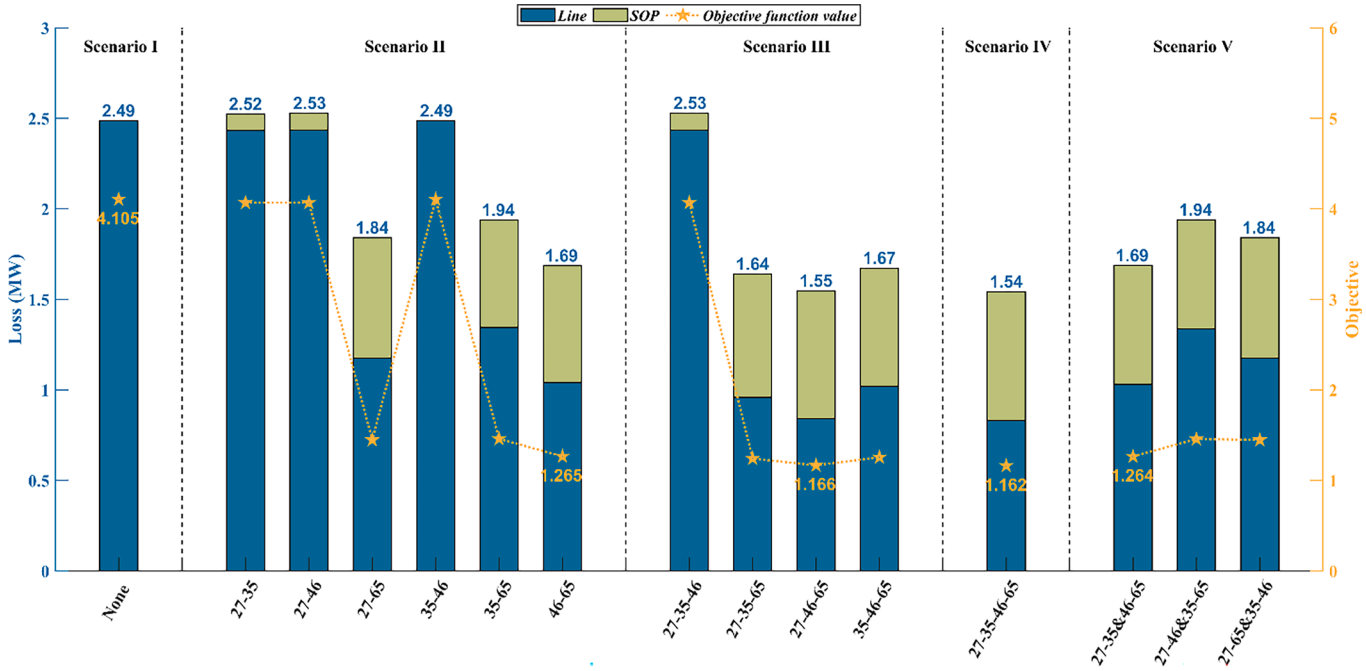

Fig. 8. Total losses and objectives in IEEE 69-node system.

TABLE 7
Results of the Optimal Installation Schemes in IEEE 69-Node System.

Scenario	MTSOP location	Objective function	Total losses (MW)	Line loss (MW)	MTSOP loss (MW)	Voltage deviation (p.u.)
I	–	4.1049	2.4867	2.4867	0.0000	8.7516
II	46–65	1.2653	1.6859	1.0412	0.6447	0.0576
III	27–46–65	1.1664	1.5474	0.8410	0.7064	0.0722
IV	27–35–46–65	1.1621	1.5423	0.8313	0.7110	0.0702
V	27–35&46–65	1.2644	1.6868	1.0312	0.6556	0.0513

TABLE 8
Results of Feasibility in IEEE 69-node system.

MTSOP location	C^{RE}($)	C^{LINE}($)	C^{MT}($)	C^{OPE}($)	δ(km)
46–65	394700	154560	54860	185280	5.0509
27–46–65	567640	207430	82290	277920	6.7789
27–35–46–65	665290	185010	109720	370560	6.0460
27–35&46–65	590790	110510	109720	370650	3.6113

network. However, under the same distribution network operation conditions, the objective function value of scheme 27–35–46–65 is 1.1621, which is only 0.37 % lower than that of scheme 27–46–65. This demonstrates that the effect improvement from Scenario III to Scenario IV is negligible and Scenario III may have already approached the optimal operating status of the system. In this status, the voltage deviation and the total losses have tended to be stable, and thus there is little room for improvement.

In terms of feasibility, Table 8 shows the corresponding feasibility results for each scheme in Table 7. When the actual length of transmission lines to be constructed for schemes 46–65, 27–46–65, 27–35–46–65 and 27–35&46–65 is less than 5.05 km, 6.78 km, 6.05 km and 3.61 km, the respective schemes are feasible. Compared to the scheme 46–65, the scheme 27–35&46–65 achieves the advantage of a lower objective function value due to multiple 2-terminal SOPs, but the higher cost of the SOPs makes it a significant reduction in the length of the transmission lines. Although the scheme 27–35–46–65 has the lowest total losses, it has a shorter transmission line length than the scheme 27–46–65 due to the higher MTSOP cost.

5.3. Modified IEEE 141-Node system

Based on the above two systems, the utilization of one 3-terminal SOP can make the distribution networks that contains four long feeders operate in a near ideal state. Here the effect of MTSOP is further tested in a system with more branches and nodes. The IEEE 141-node system with up to 6 terminals is considered, as shown in Fig. 10. Nodes 32, 52, 68, 105, 109, and 130 are the candidate installation locations of MTSOP. Node 1 is the slack bus. The rest of the parameters keep the same values in IEEE 69-node system. There are eight scenarios are considered. Table 9 shows the installation schemes of MTSOP in all scenarios.

Scenario I: No MTSOP is applied in the network.
Scenario II: One 2-terminal SOP is used for regulation.
Scenario III: One 3-terminal SOP is used for regulation.
Scenario IV: One 4-terminal SOP is used for regulation.
Scenario V: One 5-terminal SOP is used for regulation.
Scenario VI: One 6-terminal SOP is used for regulation.
Scenario VII: Two 2-terminal SOPs are used for regulation.
Scenario VIII: Three 2-terminal SOPs are used.

Fig. 11 shows the total system losses and objective values for a total of 118 schemes from Scenario I to Scenario VIII, ordered in Table 9. The results of the optimal installation schemes for Scenarios I to VIII are provided in Table 10 and the corresponding feasibility results are shown in Table 11. The maximum errors in optimal installation schemes of Scenarios I to VIII are shown in Fig. 12. Figure S3 shows the voltage changes of the optimal schemes for Scenarios I to VIII. From Fig. 12, it can be observed that these maximum errors are all at the level of 1.0e-5, indicating that the accuracy meets the requirements. Compared to Scenario I, the optimal schemes for Scenarios II to VIII have reduced objective values by 33.34 %, 46.53 %, 51.29 %, 53.53 %, 54.69 %, 51.28 %, and 54.10 %, respectively. This indicates that as the number of terminals in MTSOP increases, its capability to improve power flow distribution is also enhanced, and the performance of scheme 32–52–68–105–109–130 is the strongest, achieving the objective value of 6.0703. Besides, compared to Scenario I, the total loss of the optimal schemes for Scenarios II to VIII decreases by 15.32 %, 25.59 %, 28.26 %, 28.90 %, 28.34 %, 28.25 %, and 27.68 %, respectively. Among all the schemes, scheme 32–52–68–109–130 has the lowest total loss of 6.0299

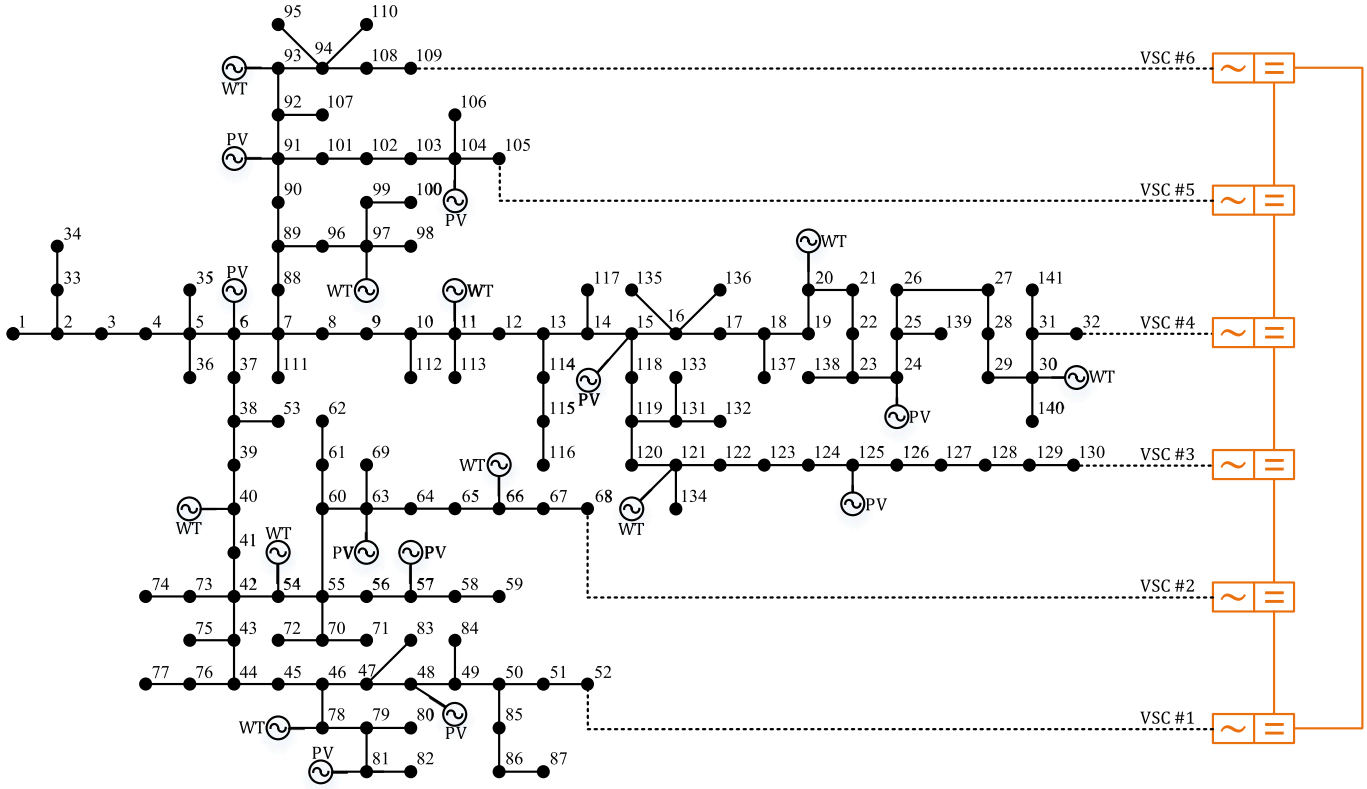

Fig. 10. Topology of MTSOP in IEEE 141-node system.

TABLE 9
Installation Locations of MTSOP in IEEE 141-Node System.

Scenario	I	II	III	IV	V	VI	VII	VIII
MTSOP location	–	32–52	32–52–68	32–52–68–105	32–52–68–105–109	32–52–68–105–109–130	32–52&68–105	32–109&105–130	32–52&68–105&109–130
	–	32–68	32–52–105	32–52–68–109	32–52–68–105–130	–	32–52&68–109	32–130&52–68	32–52&68–109&105–130
	–	32–105	32–52–109	32–52–105–109	32–52–68–109–130	–	32–52&68–130	32–130&52–105	32–52&68–130&105–109
	–	32–109	32–52–130	32–68–105–109	32–52–105–109–130	–	32–52&105–109	32–130&52–109	32–68&52–105&109–130
	–	32–130	32–68–105	52–68–105–109	32–68–105–109–130	–	32–52&105–130	32–130&68–105	32–68&52–109&105–130
	–	52–68	32–68–109	32–52–68–130	52–68–105–109–130	–	32–52&109–130	32–130&68–109	32–68&52–130&105–109
	–	52–105	32–68–130	32–52–105–130	–	–	32–68&52–105	32–130&105–109	32–105&52–68&109–130
	–	52–109	32–105–109	32–68–105–130	–	–	32–68&52–109	52–68&105–109	32–105&52–109&68–130
	–	52–130	32–105–130	52–68–105–130	–	–	32–68&52–130	52–68&105–130	32–105&52–130&68–109
	–	68–105	32–109–130	32–52–109–130	–	–	32–68&105–109	52–68&109–130	32–109&52–68&105–130
	–	68–109	52–68–105	32–68–109–130	–	–	32–68&105–130	52–105&68–109	32–109&52–105&68–130
	–	68–130	52–68–109	52–68–109–130	–	–	32–68&109–130	52–105&68–130	32–109&52–130&68–105
	–	105–109	52–68–130	32–105–109–130	–	–	32–105&52–68	52–105&109–130	32–130&52–68&105–109
	–	105–130	52–105–109	52–105–109–130	–	–	32–105&52–109	52–109&68–105	32–130&52–105&68–109
	–	109–130	52–105–130	68–105–109–130	–	–	32–105&52–130	52–109&68–130	32–130&52–109&68–105
	–	–	52–109–130	–	–	–	32–105&68–109	52–109&105–130	–
	–	–	68–105–109	–	–	–	32–105&68–130	52–130&68–105	–
	–	–	68–105–130	–	–	–	32–105&109–130	52–130&68–109	–
	–	–	68–109–130	–	–	–	32–109&52–68	52–130&105–109	–
	–	–	105–109–130	–	–	–	32–109&52–105	68–105&109–130	–
	–	–	–	–	–	–	32–109&52–130	68–109&105–130	–
	–	–	–	–	–	–	32–109&68–105	68–130&105–109	–
	–	–	–	–	–	–	32–109&68–130	–	–

MW, and the objective value is only 2.55 % higher than that of scheme 32–52–68–105–109–130. It is evident that when the number increases to five, the power flow basically reaches a stable state. In this context, when the number continues to increase to six, the line loss decreases slightly, but the MTSOP's loss increases more, resulting in a larger total loss than Scenario V. Meanwhile, the schemes that use two or three 2-terminal SOPs to interconnect multiple feeders is slightly worse than the schemes that use a single MTSOP to interconnect the same feeders simultaneously, which mainly because interconnecting multiple feeders simultaneously makes the power flow more rational. In addition, Figure S3 shows that the voltage profile improves with an increase in the number of terminals. Compared to Scenario I, the voltage deviation of the optimal schemes for Scenarios II to VIII decreased by 49.29 %, 65.07 %, 71.68 %, 75.33 %, 78.01 %, 71.68 %, and 77.49 %, respectively. In terms of voltage deviation, increasing the number of MTSOP's terminals can effectively improve the voltage quality, and the use of a single MTSOP outperforms the use of multiple 2-terminal SOPs.

Concerning the feasibility, When the actual transmission lines to be constructed for the optimal schemes of Scenarios II to VIII are less than 6.00 km, 10.19 km, 11.32 km, 11.08 km, 10.98 km, 11.36 km, and 11.21 km, respectively, the corresponding schemes are feasible. It is difficult to obtain an advantage regarding the length of transmission lines corresponding to the schemes with excellent objective function values, such as schemes 32–52–68–109–130 and 32–52–68–105–109–130. This is mainly because that once the distribution network is optimized to a certain level, the amount of variation in total loss reduction caused by increasing the number of MTSOP's terminals decreases significantly. The total loss of scheme 32–52–68–109–130 is 6.0299 MW, which only reduces 0.0543 MW compared to scheme 32–52–68–130. Scheme 32–52–68 adds a terminal on the basis of scheme 52–68, but reduces the total loss by 0.8712 MW. In this instance, the increased terminals' cost outweighs the benefit of total loss reduction, resulting in a reduction in transmission line length and a reduction in feasible geographic range.

6. Conclusion

An NLP model is developed to reveal the effect of location and topology of MTSOP in regulating distribution network's operating status. To facilitate the solution, the cone relaxation technology is applied for transforming the initial NLP model into a SOCP model. The main findings of the case study are as follows:

1) The objective values for all three system cases in this paper decrease with the increase in the number of MTSOP's terminals. Compared to the distribution network without MTSOP, the 33-node system with a 2, 3, or 4 terminal SOP decreases the objective value by up to 49.68 %, 62.28 %, and, 68.93 %, respectively. The 69-node system in the same way decreases the objective value by up to 69.18 %, 71.59 %, and 71.69 %, respectively. The 141-node system with a 2, 3, 4, 5, or 6 terminal SOP decreases the objective value by up to 33.34 %, 46.53 %, 51.29 %, 53.53 %, and 54.53 %, respectively. This indicates that as the number of MTSOP's terminals increases, its ability to improve system's operating status is also enhanced.
2) When connecting 4 feeders simultaneously, the objective value of a 4-terminal SOP scheme is 0.73 % lower than that of two 2-terminal SOP scheme in IEEE 33-node system, 8.09 % lower in IEEE 69-node system, and 0.01 % lower in IEEE 141-node system. In the case of interconnecting 6 feeders in IEEE 141-node system, the objective value of a 6-terminal SOP scheme is 1.28 % lower than that of three 2-terminal SOP schemes. The optimization results demonstrate that interconnecting multiple feeders simultaneously with MTSOP does improve the system's operating status, and both location and topology affect the effect of MTSOP significantly.
3) This paper considers using the length of the transmission line to measure the feasibility of the MTSOP's scheme. In the IEEE 33-node

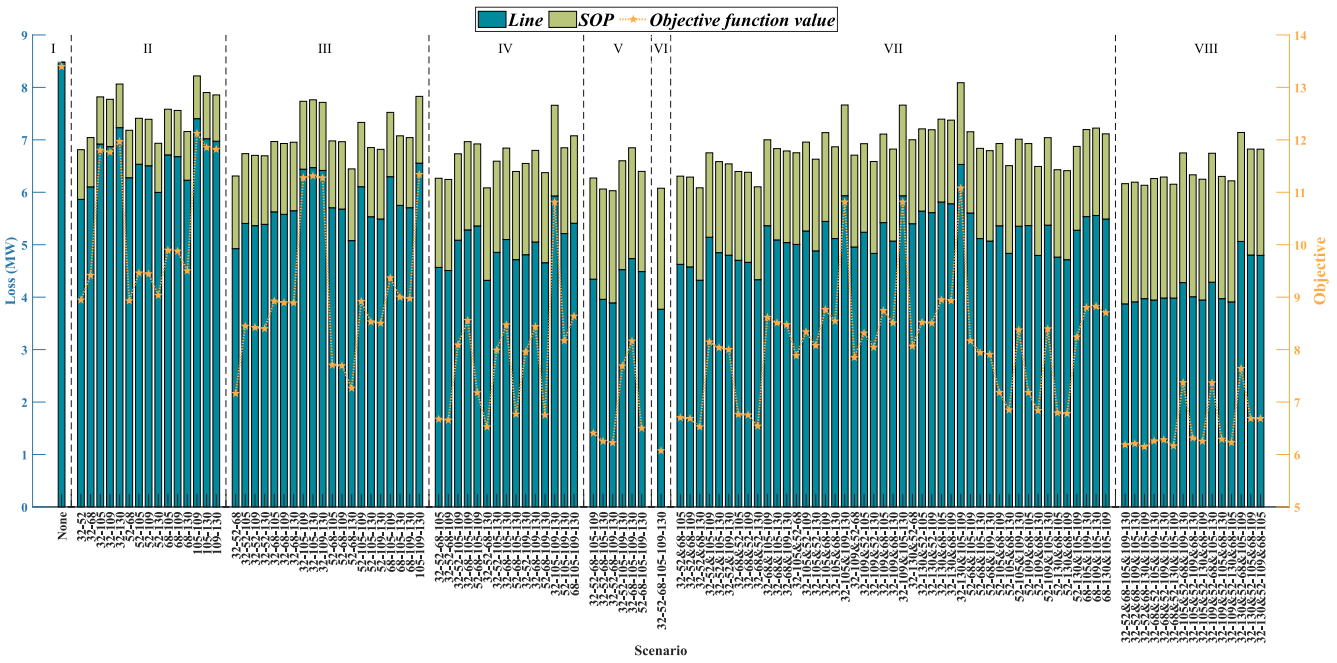

Fig. 11. Total losses and objectives in IEEE 141-node system.

TABLE 10
Results of Optimal Installation Schemes of Scenarios in IEEE 141-Node System.

Scenario	MTSOP location	Objective function	Total losses (MW)	Line loss (MW)	MTSOP loss (MW)	Voltage deviation (p.u.)
I	–	13.3966	8.4811	8.4811	0.0000	27.5116
II	52–68	8.9308	7.1821	6.2771	0.9050	13.9518
III	32–52–68	7.1632	6.3109	4.9254	1.3855	9.6105
IV	32–52–68–130	6.5253	6.0842	4.3208	1.7634	7.7920
V	32–52–68–109–130	6.2252	6.0299	3.8909	2.1390	6.7859
VI	32–52–68–105–109–130	6.0703	6.0774	3.7699	2.3075	6.0498
VII	32–52&68–130	6.5262	6.0852	4.3226	1.7626	7.7924
VIII	32–52&68–130&105–109	6.1490	6.1336	3.9712	2.1624	6.1930

TABLE 11
Results of Feasibility in IEEE 141-node system.

MTSOP location	C^{RE}($)	C^{LINE}($)	C^{MT}($)	C^{OPE}($)	δ(km)
52–68	423800	183660	54860	185280	6.0019
32–52–68	672150	311940	82290	277920	10.1941
32–52–68–130	826660	346380	109720	370560	11.3198
32–52–68–109–130	939470	339120	137150	463200	11.0825
32–52–68–105–109–130	1056300	335860	164580	555840	10.9759
32–52&68–130	827920	347640	109720	370560	11.3609
32–52&68–130&105–109	1063500	343040	164580	555840	11.2104

system, the actual transmission line length of the optimal scheme for the 2- and 4-terminal SOPs should be less than 4.38 km and 5.08 km, respectively. In IEEE 69-node system, the actual transmission line length of the optimal scheme for SOP with 2, 3, or 4 terminals needs to be less than 5.05 km, 6.78 km, and 6.05 km. In the 141 node system, the actual transmission line length of the optimal scheme for SOP from 2 to 6 terminals needs to be less than 6.00 km, 10.19 km, 11.32 km, 11.08 km, and 10.98 km. It is evident that the SOPs with a large number of terminals are difficult to gain an advantage in feasibility because when the distribution network is optimized to a certain level, the cost of increasing terminals is greater than the electricity cost saved by reducing system losses, resulting in a decrease in feasibility.

4) Based on the above conclusion, the selection of the MTSOP's topology should take into account not only the scale of the distribution network, but also the geographical location of the distribution network. On the one hand, the larger the distribution network, the greater the number of MTSOP's terminals required to adequately improve the operational status of the distribution network. On the other hand, the greater the number of MTSOP's terminal, the more complicated it is to implement, so the topology and location of the MTSOP must be chosen based on the geographic location. Besides, as the number of MTSOP's terminal increases, the system's operating status is also improved. When the quantity of terminals reaches a certain point, the improvement decreases dramatically, mainly because the system is already operating at an almost optimal level. In this case, continuing to increase the number of MTSOP's terminals has little effect on reducing system total losses, and even increases them instead. Therefore, considering the scale of the distribution network, feasibility, performance, control complexity, and cost of

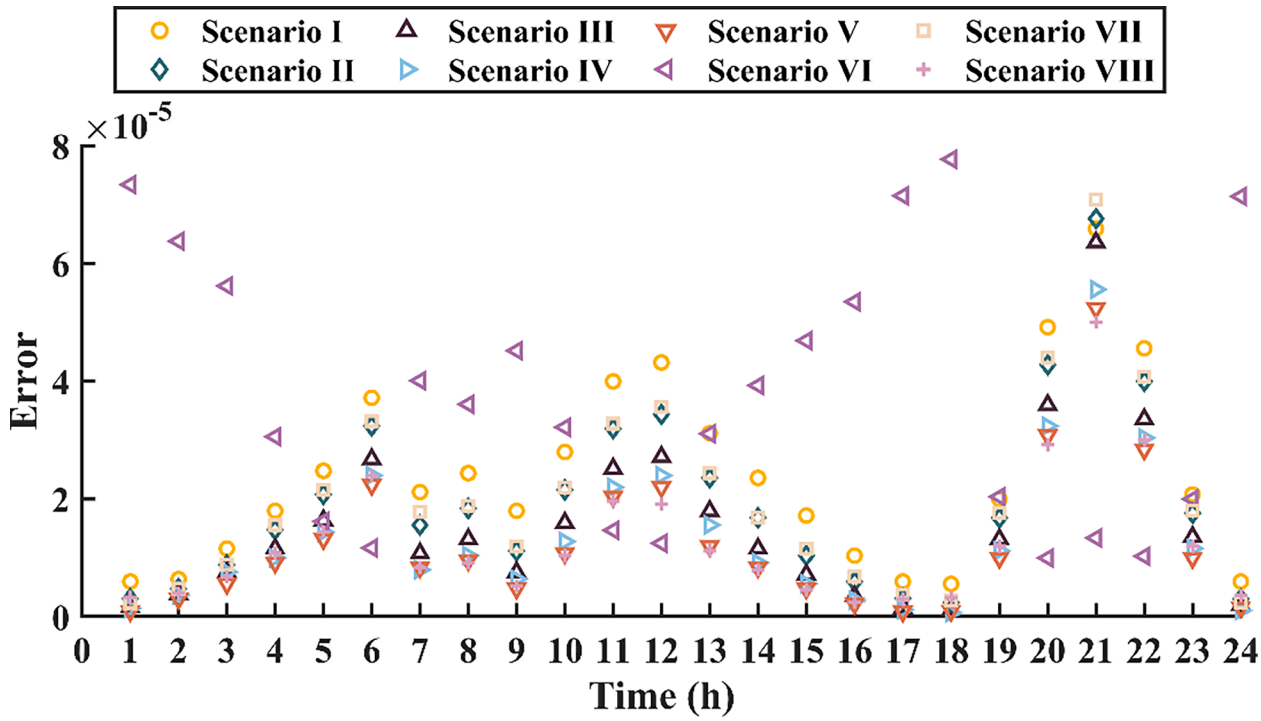

Fig. 12. Maximum errors in optimal installation schemes of Scenarios I to VIII (IEEE 141-node system).

MTSOP, the number of terminals is not as high as possible, and the corresponding number of terminals and their installation locations need to be determined according to the characteristics of the network.

The limitations of this paper and future research directions are as follows:

1) We only consider the MTSOP installed at the end of feeders, which does not necessarily maximize its usefulness. In the future, we will expand the installation location to the inside of the feeders, and search for the optimal topology and installation location of MTSOP globally in a larger distribution network to enhance the scalability of the optimization framework.
2) The solution method used in this paper is widely applied in the optimization of distribution networks, but there are limitations in solving large-scale distribution systems. Improving the accuracy and computational efficiency of algorithms is of great help for optimizing SOP configuration. Therefore, future research can consider improving the algorithm to support SOP in selecting the optimal topology and location globally in the distribution network.

CRediT authorship contribution statement

Haibo Zhou: Writing – original draft, Software, Methodology. **Guojiang Xiong:** Writing – review & editing, Supervision, Project administration, Formal analysis. **Xiaofan Fu:** Writing – review & editing, Validation, Formal analysis, Data curation. **Man-Chung Wong:** Writing – review & editing, Formal analysis, Conceptualization. **Louis-A. Dessaint:** Formal analysis, Conceptualization. **Kamal Al-Haddad:** Formal analysis, Conceptualization.

Declaration of competing interest

The authors declare that they have no known competing financial interests or personal relationships that could have appeared to influence the work reported in this paper.

Acknowledgments

This research was funded by the National Natural Science Foundation of China (52167007), the Natural Science Foundation of Guizhou Province (QiankeheBasic-ZK[2022]General121), and the Modern Power System and Its Digital Technology Engineering Research Center (QianJiaoJi[2022]043).

Appendix A. Supplementary material

Supplementary data to this article can be found online at https://doi.org/10.1016/j.ijepes.2025.110721.

Data availability

Data will be made available on request.

References

[1] Zhu JH, Ren HF, Gu JP, Zhang XS, Sun CX. Economic dispatching of Wind/photovoltaic/ storage considering load supply reliability and maximize capacity utilization. Int J Electr Power Energy Syst 2023;147:108874.
[2] Chen HP, Wu H, Kan TY, Zhang JH, Li HL. Low-carbon economic dispatch of integrated energy system containing electric hydrogen production based on VMD-GRU short-term wind power prediction. *Int J Electr Power Energy Syst* 2023;154:109420.
[3] Rahman DM, Ganguly S. Voltage regulation and energy loss minimization for distribution networks with high photovoltaic penetration and EV charging stations using dual-stage model predictive control. *Sustain Energy Grids* 2024;40:101529.
[4] Azeredo LFS, Yahyaoui I, Fiorotti R, Fardin JF, Garcia-Pereira H, Rocha HRO. Study of reducing losses, short-circuit currents and harmonics by allocation of distributed generation, capacitor banks and fault current limiters in distribution grids. *Appl Energy* 2023;350:121760.
[5] Rossi M, Vigano G, Rossini M. Linear optimal power flow model for modern distribution systems: management of normally closed loop grids and on-load tap changers. *Electr Power Syst Res* 2024;235:110653.
[6] Sun XZ, Qiu J, Tao YC, Ma Y, Zhao JH. A multi-mode data-driven volt/var control strategy with conservation voltage reduction in active distribution networks. *IEEE Trans Sustain Energy* 2022;13(2):1073–85.
[7] Cao WY, Wu JZ, Jenkins N. Feeder load balancing in MV distribution networks using soft normally-open points. In: IEEE PES Innovative Smart Grid Technologies Conference Europe, Istanbul, Turkey; 2014. p. 1–6.

[8] Behbahani MR, Jalilian A. Optimal operation of soft open point devices and distribution network reconfiguration in a harmonically polluted distribution network. *Electr Power Syst Res* 2024;237:110967.
[9] Wang P, Li HW. Coordinated planning of soft open point and energy store system in active Distribution networks under source-load imbalance. *Electr Power Syst Res* 2024;231:110324.
[10] Wang CS, Song GY, Li P, Ji HR, Zhao JL, Wu JZ. Optimal siting and sizing of soft open points in active electrical distribution networks. *Appl Energy* 2017;189:301–9.
[11] Guo XM, Huo QH, Wei TZ, Yin JY. A local control strategy for distributed energy fluctuation suppression based on soft open point. *Energies* 2020;13(6).
[12] Jiang X, Zhou Y, Ming WL, Yang P, Wu JZ. An overview of soft open points in electricity distribution networks. *IEEE Trans Smart Grid* 2022;13(3):1899–910.
[13] Yang XD, Zhou ZY, Zhang YB, Liu JC, Wen JY, Wu QW, et al. Resilience-oriented co-deployment of remote- controlled switches and soft open points in distribution networks. *IEEE Trans Power Syst* 2023;38(2):1350–65.
[14] Zhang W, Zhang C, Li JY, Cao SR, Wang DP, Yang HZ, et al. Resilience-oriented comparative study of SOP-based service restoration in distribution systems. *Electr Power Syst Res* 2024;228:110050.
[15] Li P, Ji J, Ji HR, Song GY, Wang CS, Wu JZ. Self-healing oriented supply restoration method based on the coordination of multiple SOPs in active distribution networks. *Energy* 2020;195:116968.
[16] Ji HR, Wang CS, Li P, Song GY, Wu JZ. SOP-based islanding partition method of active distribution networks considering the characteristics of DG, energy storage system and load. *Energy* 2018;155:312–25.
[17] Zhang JR, Foley A, Wang SY. Optimal planning of a soft open point in a distribution network subject to typhoons. *Int J Electr Power Energy Syst* 2021;129:106839.
[18] Wang J, Zhou NC, Chung CY, Wang QG. Coordinated planning of converter-based DG units and soft open points incorporating active management in unbalanced distribution networks. *IEEE Trans Sustain Energy* 2020;11(3):2015–27.
[19] Sarantakos I, Zografou-Barredo NM, Huo D, Greenwood D. A reliability-based method to quantify the capacity value of soft open points in distribution networks. *IEEE Trans Power Syst* 2021;36(6):5032–43.
[20] Sun FZ, Ma JC, Yu M, Wei W. Optimized two-time scale robust dispatching method for the multi-terminal soft open point in unbalanced active distribution networks. *IEEE Trans Sustain Energy* 2021;12(1):587–98.
[21] Ma DJ, Chen W, Shu LC, Qu XH, Gao SL, Hou K. A multiport AC–AC–DC converter for soft normally open point. *IEEE Trans Circuits Syst II Express Briefs* 2022;69(4):2146–50.
[22] Taher AM, Hasanien HM, Alsaleh I, Aleem SHEA, Alassaf A, Almalaq A. Optimizing active distribution microgrids with multi-terminal soft open point and hybrid hydrogen storage systems for enhanced frequency stability. *J Energy Storage* 2024;99:113369.
[23] Abdelrahman MA, Long C, Wu JZ, Jenkins N. Optimal operation of multi-terminal soft open point to increase hosting capacity of distributed generation in medium voltage networks. In: *2018 53rd International Universities Power Engineering Conference (UPEC), Glasgow, UK*; 2018. p. 1–6.
[24] Zhang JW, Feng X, Zhou JQ, Zang JJ, Wang JC, Shi G, et al. Series–shunt multiport soft normally open points. IEEE Trans Ind Electron 2023;70(11):10811–21.
[25] Xiao TT, Peng YG, Chen CY. A temporal and spatial electric vehicle charging optimization scheme with DSO-EVA coordination framework. *Int J Electr Power Energy Syst* 2024;156:109761.
[26] Zhao YD, Xiong W, Yuan XF, Zou XS. A fault recovery strategy of flexible interconnected distribution network with SOP flexible closed-loop operation. *Int J Electr Power Energy Syst* 2022;142:108360.
[27] Li P, Ji HR, Wang CS, Zhao JL, Song GY, Ding F, et al. Coordinated control method of voltage and reactive power for active distribution networks based on soft open point. *IEEE Trans Sustain Energy* 2017;8(4):1430–42.
[28] Saaty TL. Decision making — the analytic hierarchy and network processes (AHP/ANP). *J Syst Sci Syst Eng* 2004;13(1):1–35.
[29] Baran ME, Wu FF. Optimal capacitor placement on radial distribution systems. *IEEE Trans Power Deliv* 1989;4(1):725–34.
[30] Andersen ED, Roos C, Terlaky T. On implement a primal-dual interior point methods for conic quadratic optimization. *Math Program* 2003;95(2):249–77.
[31] Huang C, Li FX, Ding T, Jin ZQ, Ma X. Second-order cone programming-based optimal control strategy for wind energy conversion systems over complete operating regions. *IEEE Trans Sustain Energy* 2015;6(1):263–71.
[32] Gan LW, Li N, Topcu U, Low SH. Exact convex relaxation of optimal power flow in radial networks. *IEEE Trans Autom Control* 2015;60(1):72–87.

HaiboZhou received the B.Sc. degree from Guizhou University, Guiyang, China, in 2022. He is now pursuing the M.Sc. degree in the College of Electrical Engineering, Guizhou University, Guiyang, China. His main research interests include optimal operation of flexible distribution network.

Guojiang Xiong received the B.Sc. degree from Zhejiang University, Hangzhou, China, in 2009, and the M.Sc. and Ph.D. degrees from Huazhong University of Science and Technology (HUST), Wuhan, China, in 2011 and 2014, respectively. From August 2014 to August 2017, he was an engineer with the Guizhou Electric Power Grid Dispatching and Control Center, Guiyang, China. After that, he joined the College of Electrical Engineering, Guizhou University (GZU), as an Associate Professor. Since January 2019, he has been a Distinguished Professor at GZU. He has published over 80 research papers in journals and been a reviewer for over 30 journals and conferences. His main research interests include renewable energy, power system operation, fault diagnosis of power system, and application of artificial intelligence in power systems.

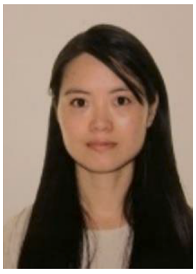

XiaofanFu (M'16) received the B.Eng. degree in electrical engineering from Taiyuan University of Technology, Taiyuan, China, in 2003; received the M.Eng. degree in electrical engineering from Guizhou University, Guiyang, China, in 2006; from 2006 to 2009, had the systematic Ph.D. study in electrical engineering from Southeast University, Nanjing, China; and received the Ph.D. degree in electrical engineering from École de Technologie Superieure, University of Quebec, Montreal, Canada, in 2016. From January 2017 to August 2019, she worked as a postdoctoral researcher in GREPCI lab of École de Technologie Superieure, University of Quebec, Montreal, Canada. From 2019 to 2020, she worked as a postdoctoral research Fellow in the State Key Laboratory of Internet of Thing Smart City, University of Macau, Macao, China. She is currently a lecturer with the School of Electrical engineering, Guizhou University, Guiyang, China. Her research interests include voltage-source converter family of HVDC, grid integration of renewable energy, and microgrid technology.

Man-Chung Wong (SM'06) received the B.Sc. and M.Sc. degrees in Electrical and Electronics Engineering from the University of Macau (UM), Macao, China, in 1993 and 1997, respectively; and received his Ph.D. degree in Electrical Engineering from Tsinghua University, Beijing, P. R. China, in 2003. Currently, he is a professor and the department head in the Department of Electrical and Computer Engineering at the University of Macau. He was a visiting fellow at Cambridge University. Now he is affiliated with the State Key Laboratory of Internet of Things for Smart City and the State Key Laboratory of Analog and Mixed Signal VLSI, University of Macau, Macao, China. He published four books and more than 180 technical journals (more than 70 SCI papers) and conference papers and holds four U.S. patents and 8 Chinese patents. He has four U.S. and 8 Chinese patents. His research interests include integrated power electronics controllers, power electronics converters, power quality compensators, renewable energy, wireless power transfer, and smart grid. Prof. Wong was a recipient of Second Class 2022 Macao Science and Technology Natural Science Award, the Macao Science and Technology Invention Awards (2nd Class in 2018, 3rd Class in 2014 and 2012, respectively), and the Young Scientist Award from "Instituto Internacional De Macau" at 2000, Young Scholar Award from University of Macau at 2001, Second Prize of 2003 Tsinghua University Excellent Doctor Thesis Award. He was IEEE TENCON Macao 2015 General Chair and IEEE APPEEC Macao 2019 General Chair. He was Chair of the IEEE Macau Section in 2014- 2015, and he was a chair of the IEEE Macau PES/PELS Joint Chapter between 2015 and 2020. He has been an IEEE Region 10 Power and Energy Society North Representative since 2015.

Louis-A. Dessaint (M'88–SM'91–F'13–LF'20) received the B. Ing., M.Sc.A., and Ph.D. degrees from the Ecole Polytechnique de Montreal, Universite du Quebec, Montreal, QC, Canada, in 1978, 1980, and 1985, respectively, all in electrical engineering. He is currently a Professor at the Ecole de Technologie Superieure, Université du Québec in Montréal. He is an author of the The MathWorks "SimPowerSystems" (SPS) Blockset. He was also an Associate Editor of the IEEE Transactions on Control Systems Technology and IET Generation, Transmission and Distribution. Dr. Dessaint is a Fellow of the Canadian Academy of Engineering and a member of the Cercle of Excellence of the University of Quebec.

Kamal Al-Haddad (S'82–M'88–SM'92–F'07–LF'19) received the B.Sc.A. and M.Sc.A. degrees in electrical engineering from the University of Québec à Trois-Rivières, Canada, in 1982 and 1984, respectively, and the Ph.D. degree in electrical engineering from the Institute National Polytechnique, Toulouse, France, in 1988. Since 1990, he has been a Professor with the Electrical Engineering Department, École de Technologie Supérieure (ÉTS), Montreal, QC, Canada, where he has been the Canada Research Chair in Electric Energy Conversion and Power Electronics, since 2002. He has supervised more than 170 Ph.D. and M.Sc.A. students working in the field of power electronics. He is a consultant and has established very solid link with Canadian industries. He has coauthored more than 600 transactions and conference papers and two books. His research interests include high-efficient static power converters, active-hybrid power filters, grid connect, and multilevel converters, including modeling, control, and development of prototypes for various industrial applications. Professor Al-Haddad is a member of the Academy of science, a Fellow of the Royal Society of Canada, and a Fellow Member of the Canadian Academy of Engineering. He was a recipient of the Dr.-Ing. Eugene Mittelmann Achievement Award. He was the IEEE IES President, from 2016 to 2017, and is an IES Distinguished Lecturer and the recipient of the Dr.-Ing. Eugene Mittelmann Achievement Award.